



Solar Household Energy, Inc.

Solar Cooking for Human Development and Environmental Relief

SHE Technical Report no. TR-31

Measuring Solar Radiation with a Sun Tracker for the Solar Cooker Power Standard

Everest Bloomer* and Paul Arveson**

**Blair High School*

***Solar Household Energy, Inc.*

October 30, 2017

Citation: Technical Report no. TR-31, Solar Household Energy, Inc., (Oct. 30, 2017)

Copyright © 2017, Solar Household Energy, Inc. and Everest Bloomer.

Solar Household Energy (SHE) strives to unleash the potential of solar cooking to improve social, economic and environmental conditions in sun-rich areas around the world. SHE Technical Reports are intended for use within the solar cooking community, for the rapid dissemination of findings related to solar cookers. They may contain information that is based on limited data, and/or conclusions and recommendations that are solely the opinions of the author, not of the organization. Please contact the author for further correspondence.

Abstract

Billions of people still depend on food cooked over an open fire. This ancient practice has many serious health and environmental consequences. It is estimated that annually 3.5 million deaths of women and children die from exposure to cooking smoke. Currently an International Standards Organization is developing a standard to define protocols for measuring the performance of improved cookstoves of all types. This includes solar cookers, which release no emissions, use no fuels, and can reduce fuel costs for low-income people and refugees. In the US there is an existing standard for solar cooker power. We constructed instrumentation required to measure power, and we constructed a Sun tracker to automate measurement of solar radiation. This provides an accurate and convenient way to improve the measurements.

Introduction

About 2.7 billion people currently depend on an open fire or an inefficient cookstove to cook food [1]. The ancient practice of using wood or charcoal for cooking has many serious consequences, including deforestation, habitat loss, soil erosion, burns, and the excessive and dangerous labor of gathering and chopping wood, which prevents women (the large majority of cooks) from opportunities for education or employment. But the most acute consequence of biomass cooking is the health impacts of emissions near the cooking fire. The World Health Organization (WHO) estimates that around 6.5 million premature deaths each year can be attributed to air pollution. In fact, the number of deaths attributed to air pollution each year is much greater than the number from HIV/AIDS, tuberculosis, and road injuries combined. Around 3.5 million of these deaths are caused by respiratory diseases of women and small children exposed every day to cooking smoke [2].

In 2013, US leaders from the Environmental Protection Agency's Partnership for Clean Indoor Air and the Department of Energy (DOE) met in Washington to recruit a team of interested scientists to support the development of an international standard for "Clean Cookstoves and Clean Cooking Solutions" [4]. The groups are developing protocols for measurement of power, efficiency, emissions, durability, safety, and user acceptance of cookstoves. The work now involves experts from over 25 countries. The scope covers all types of household-scale devices for cooking food and heating water, and all energy sources [6].

Solar cookers (or cookstoves) are of particular interest to the authors. They have no emissions, use no fuels, and can have a low total cost of ownership. They are especially suitable in regions where there is ample solar radiation (insolation). Many of these locations, including most refugee camps, are in sub-Saharan Africa, the Middle East, India, and northern China.

Solar thermal cookers use concentrated sunlight to heat food. They do not use photovoltaic (PV) technology. They are simple, "low-tech" devices that come in a wide variety of designs. The three main types of solar cookers that are in common use are:

- Panel cookers, which use an arrangement of flat or curved reflectors aimed at a black cooking pot, with a transparent cover around the pot to reduce heat loss.
- Box cookers, which use an insulated box with a window on top and one or more flat reflectors aimed into the box.
- Parabolic cookers, which use a doubly-curved mirror that focuses concentrated sunlight onto the cooking vessel.

Panel and box cookers are low-power devices that operate like an electric slow cooker (e.g. the "Crock PotTM"), whereas parabolic cookers are high-power devices that are suitable for fast stir-fry cooking at high temperatures. A comprehensive catalog of solar cooker designs has been compiled [7].

A Washington DC-based nonprofit organization, Solar Household Energy (SHE), leverages the power of solar cooking to improve social, economic and environmental conditions in sun-rich areas around the world. Since 1998, Solar Household Energy has worked with non-governmental organizations, entrepreneurs and public sector entities to promote solar cooking with modern solar ovens, including the "HotPot" developed by SHE. The organization helps to introduce the technology in developing countries through making suitable devices available within the context of comprehensive training initiatives, including progress monitoring and project evaluation.

The Solar Cooker Power Standard

In order to advance the acceptance of solar cookers, it is necessary to include them within the international standard for cooker power, so that countries can assess and compare different devices in a credible and fair manner. Several countries already have developed national standards for measuring the performance (i.e. power and efficiency) of solar cookers. In the US the standard is ASAE (American Society of Agricultural Engineers) S580.1 [10].

This standard results in a single measure of performance, namely cooking power in Watts. A solar cooker extracts some of the sun's power (in Watts per square meter) and concentrates this sunlight onto a pot, where some of it is absorbed in heating the food. Therefore, it is necessary to accurately measure the incoming sunlight, which varies depending on the motion of the Sun across the sky, the presence of clouds, and air quality.

One of the projects at SHE is the development of a testing system to measure and evaluate solar cookers. Currently one of the authors (Arveson) has developed a testing system using a pyranometer and other instruments, to measure solar cooker power in accordance with the ASAE standard.

Features of solar radiation

Dr. David R. Brooks described the basic facts of solar radiation:

"At Earth's distance from the sun, an average of about 1370 W/m^2 of power reaches the top of the Earth/atmosphere system. About 30% is reflected back to space, mostly by clouds. About 70% is absorbed by Earth's surface and atmosphere and is then re-radiated in the form of thermal radiation. Around midday on a summer day in temperate climates, roughly 1000 W/m^2 of power reaches Earth's surface. This is a lot of power, even when the available energy is averaged over a day! "

During a day, sunlight comes directly from the sun, but also scatters off surrounding clouds and the sky. Sunlight is quantified as irradiance - the rate at which radiant energy arrives at a specific area of surface during a specific time interval. A typical unit is Watts per square meter (W/m^2). Scientists divide solar irradiance into three parts:

1. Direct Normal Irradiance (DNI) - a synonym for beam radiation, the amount of solar radiation from the direction of the sun.

2. Diffuse Horizontal Irradiance (DHI) - a synonym for diffuse sky radiation.

Diffuse Sky Radiation - the radiation component that strikes a point from the sky, excluding circumsolar radiation. In the absence of atmosphere, there should be almost no diffuse sky radiation. High values are produced by an unclear atmosphere or reflections from clouds.

3. Global Horizontal Radiation (GHI) - also called Global Horizontal Irradiance; total solar radiation; the sum of Direct Normal Irradiance (DNI), Diffuse Horizontal Irradiance (DHI), and ground-reflected radiation; however, because ground reflected radiation is usually insignificant compared to direct and diffuse, for all practical purposes global radiation is said to be the sum of direct and diffuse radiation only:

$$GHI = DHI + DNI * \cos (Z)$$

where Z is the solar zenith angle.

Solar cookers of all types use a reflector to concentrate sunlight in order to cook food. The only light that can be concentrated is the DNI (direct normal irradiance), which reflects in a controlled way based on Snell's Law (angle of incidence = angle of reflection). The diffuse component of sunlight comes from random directions, and thus cannot be concentrated by reflectors. So only the DNI is relevant to solar cooker power.

Even on a clear day, the DNI is not constant as the Sun moves across the sky. The main reason for this is the variation in airmass. Airmass is the relative path length of the direct sunlight

through the atmosphere. When the Sun is directly above a sea-level location the path length is defined as airmass 1 (AM 1.0). AM 1.0 is not synonymous with solar noon because the Sun is usually not directly overhead at solar noon in most seasons and locations. When the angle of the Sun from zenith (directly overhead) increases, the airmass increases approximately by the secant of the zenith angle.

This figure below illustrates the concept of airmass:

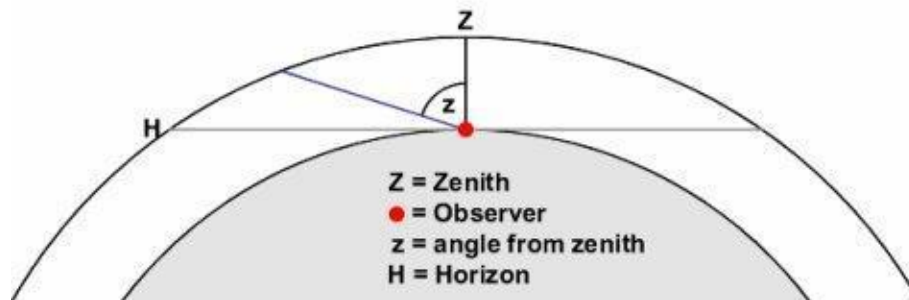


Figure 1: Airmass is proportional to the distance that sunlight passes to reach an observer, depending on the zenith angle (Z) to the Sun.

The following figure shows a typical set of measurements of DNI, DHI and GHI on a clear day in Tucson, Arizona (Oct. 27, 2017).

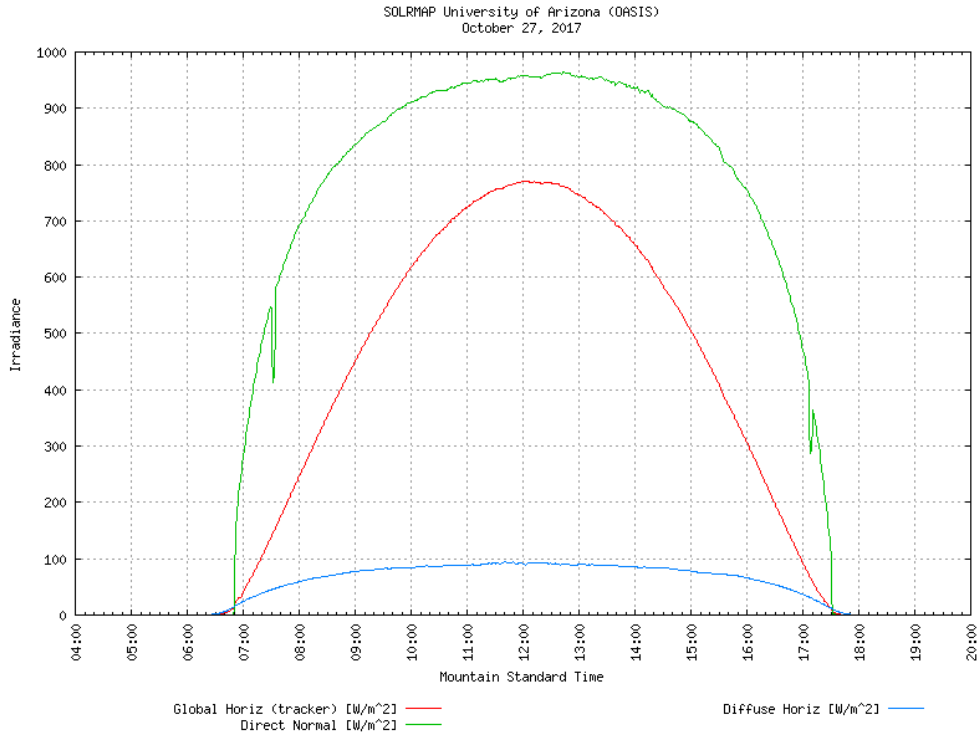


Figure 2: GHI (red), DNI (green) and DHI (blue) for a clear day in Tucson, Arizona.

Clouds cause significant drops in the levels of solar radiation. The following figure shows an example of irradiance measurements on a partly cloudy day:

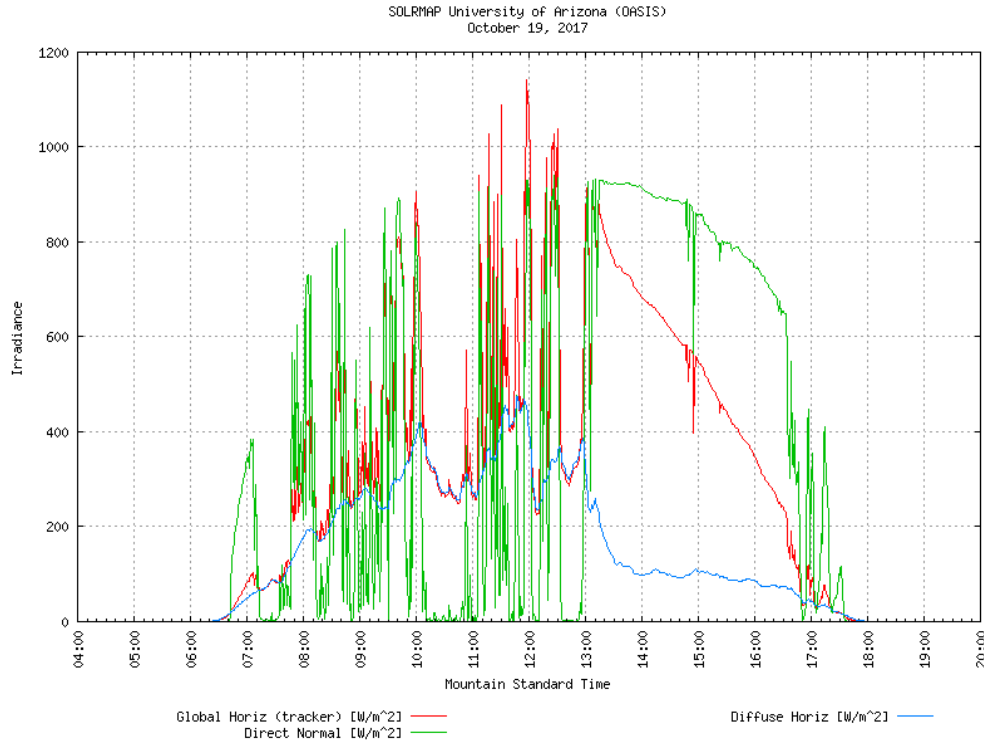


Figure 3: GHI, DNI and GDI measurements on a partly cloudy day in Tucson, Arizona

In this example, note that the average irradiance is significantly lowered during the cloudy times in the morning. The GHI (red curve) sometimes is even higher than the DNI (green curve), which has a maximum of about 900 W/m². This may be caused by Mie scattering of light from clouds near the Sun. However, this radiation is not useful for solar cooking because it is diffused rather than direct radiation, so it cannot be focused with reflectors. On this particular day, solar cooking would only be feasible in the afternoon.

Measuring solar irradiance

Instruments used to measure irradiance are called pyranometers (from the Greek *pyr* (fire) and *ano* (sky)). Ideally, pyranometers should measure all the radiation from the sun, across the entire electromagnetic spectrum (broadband radiation). Pyranometers based on thermopile detectors (collections of thermocouples embedded in special materials) closely approach this ideal.

However, such instruments cost several thousand dollars. Much less expensive pyranometers – what might be called "surrogate" pyranometers – use miniature silicon solar cell detectors, which are primarily sensitive to red and near-infrared light.

The pyranometer used in SHE's testing system is an Apogee SP-212 powered silicon solar cell detector. [ref] This is a small but accurate instrument that is suitable for general use in solar measurements. Such pyranometers have a "cosine" angle response, meaning that the output is proportional to the cosine of the angle between the Sun direction and the centerline axis of the pyranometer.



Figure 4: Apogee pyranometer in leveling mount for measuring GHI.

Normally, such pyranometers are mounted pointing vertically, so their response is highest at the zenith angle (directly overhead). Here is a photo showing a collection of pyranometers mounted in the calibration lab at National Renewable Energy Laboratory in Colorado.



Figure 5: Pyranometers in NREL testing lab.

Thus, when mounted vertically, solar irradiance measurements have a zenith angle dependence that is the product of the cosine response of the sensor times the airmass thickness, which means that the net response goes approximately as cosine-squared (zenith angle). Figure 6 illustrates this function.

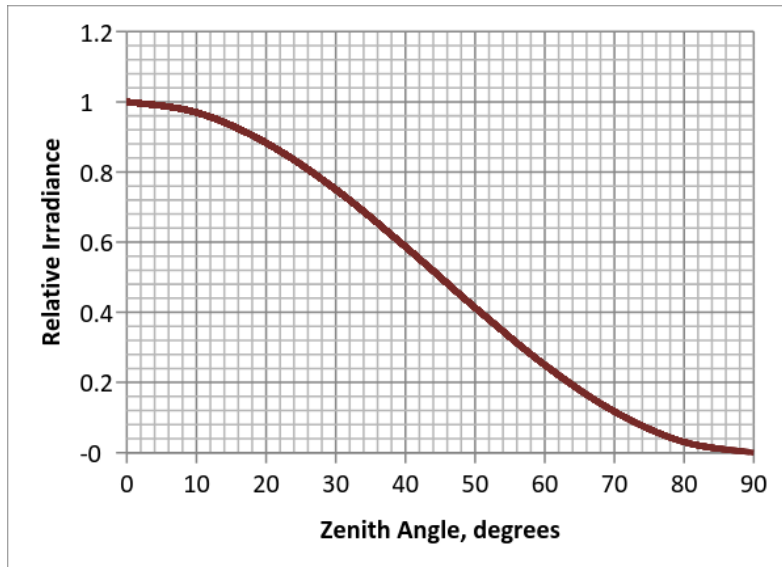


Figure 6: Theoretical dependence of irradiance on zenith angle.

Using a vertically-pointing pyranometer, it is possible to calculate the DNI if we know the altitude of the Sun. If that is known, we can simply adjust for the cosine angle response of the pyranometer. But calculating the sun's zenith angle as a function of time during the day is an astronomy problem. It depends on the latitude of the measurement location, the time of day, and the day of the year. This is a complicated calculation, and it is also sensitive to deviations in the cosine response of the pyranometer.

Materials and Methods

The astronomical complexities with the zenith angle affecting irradiance can be avoided simply by measuring the direct normal irradiance of the Sun using a Sun tracker. In this case, no astronomical calculations are necessary to measure the incident power to the solar cooker being tested. We simply measure it directly.

In fact, this is actually what is called for in the ASAE S.580.1 standard: "Available solar energy shall be measured in the plane perpendicular to direct beam radiation (the maximum reading) using a radiation pyranometer." This requires pointing the pyranometer toward the Sun during the measurements.

A search on the Internet identified several low-cost Sun tracker construction projects and kits. We selected one of them that has robust synchros and a platform that can be used for mounting pyranometers. The tracker was based on a circuit that matches the voltage across four cadmium sulfide photoresistors.

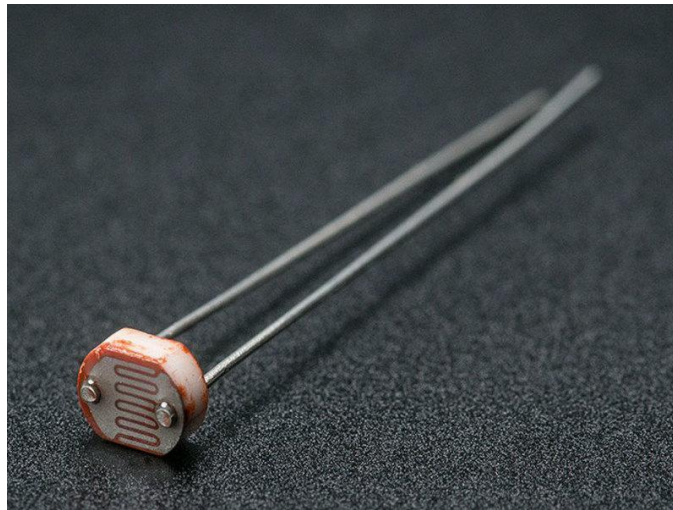


Figure 7: A cadmium sulfide photoresistor.

The kit selected was RobotGeek's Solar Tracker project, based on their "RoboTurret" design. The RoboTurret operates with an Arduino controller mounted with a sensor shield.

Servos were centered before construction of the base RoboTurret. The horns were mounted to the servos and the side bracket was attached to the active horn of the pan servo. 4 Hex Socket Head Bolt M2 x 5 were used to attach the bracket to the horn. The tilt servo was attached to the side bracket on the pan servo using 4 Hex Socket Head Bolt M2 x 5 and 4 Hex Nut M2. The nut holder tool was used to help connect both servos to each other. The C bracket was attached to the tilt servo with 6 Hex Socket Head Bolt M2 x 5, three into each horn. The following figure shows what the RoboTurret looked like at this stage.



Figure 8: The servos attached to the top plate

Attached to the Arduino were 3 Hex Standoff F/F M3 x 10 using 3 Washer M3 and 3 Hex Socket Head Bolt M3 x 6. Then the Arduino was mounted to the top plate on the Standoffs using another 3 Washer M3 and 3 Hex Socket Head Bolt M3 x 6. The Sensor Shield was attached right

on top of the Arduino. The figure below shows the Arduino attached to the bottom of the Top Plate.



Figure 9: The Arduino and Sensor Shield attached to the Top Plate

The Bottom Plate was attached to the Top Plate using 4 Hex Standoff M/F M3 x 15 attached to 4 Hex Standoff F/F M3 x 30, and those were attached between the Top Plate and the Bottom plate with 4 Hex Socket Head Bolt M3 x 6 for each side. 6 Large Rubber Bumpers were attached to the bottom side of the Bottom Plate. The Servos were then wired through the gaps between the Arduino and the Sensor Shield to help against tangling up with cords, and the servos were plugged into the Arduino. Figure 10 shows the Turret up to this point.



Figure 10: The RoboTurret without the mounted plates

An extra 90 Degree Power Cable was attached to the Arduino and fed under the Bottom Plate to allow for easier power supplying, and the 90 Degree Power Cable was held in place by two zip ties. The Top Mount plate was attached directly to the C Bracket on the tilt servo using 4 Hex Socket Head Bolt M2 x 6 and 4 Nut M2. On the Top Mount plate, a larger Placement Plate was attached using 4 Hex Standoff M3 x 10 and 8 Hex Socket Head Bolt M3 x 6, 4 for each side to attach the plate. The Placement Plate was divided into 4ths by 2 sheets of aluminum, painted

with black paint. In each quadrant, a RobotGeek light Sensor was attached using the enclosed standoffs. On the Bottom Plate, 2 RobotGeek rotation knobs were attached, and they were attached to the Arduino using six 3 wire connectors. See Figure 14 for the completed solar tracker. The Arduino open source code for the solar tracker was downloaded from the *hackster.io* website [11].

Results

October 27, 2017 was an exceptionally clear day in Rockville, MD, so the tracker was set out in the Sun and the pyranometer was attached to the tracker platform. The data logger was started at 11:03am and the instruments were left alone for the day. Figure 11 shows the resulting data.

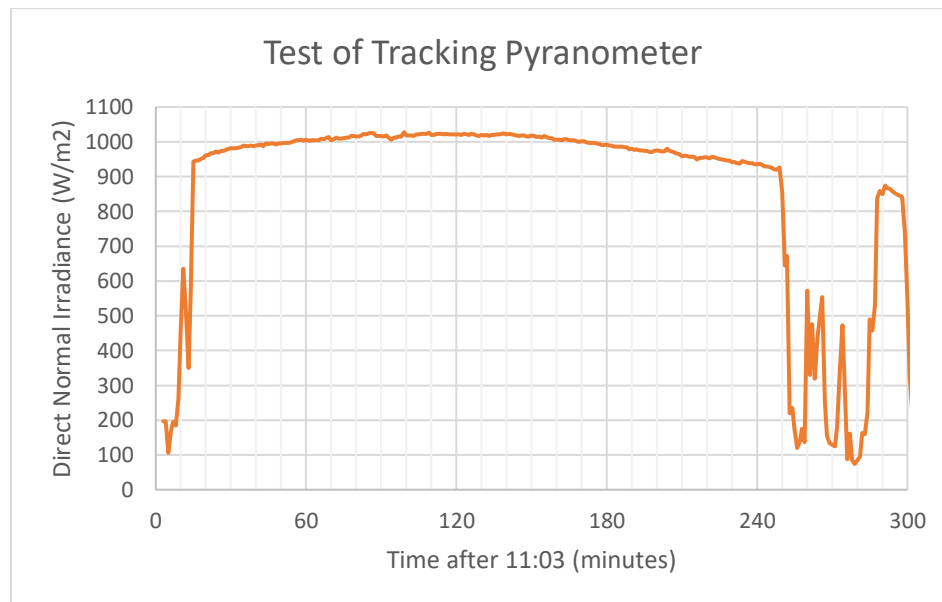


Figure 11: First test measurements of DNI with pyranometer on Sun tracker.

These data indicate that the tracker followed the Sun all day, unattended. The dropouts near the beginning of the data were due to measurements acquired before the instruments were set in

sunlight. The variations after 240 minutes were due to trees that blocked the direct sunlight later in the day.

To check the overall curve of Direct Solar Irradiance (DNI), these data were compared to clear-sky measurements in Tucson, Arizona, where The National Renewable Energy Laboratory (NREL) has an online instrument system that reports solar irradiance daily.

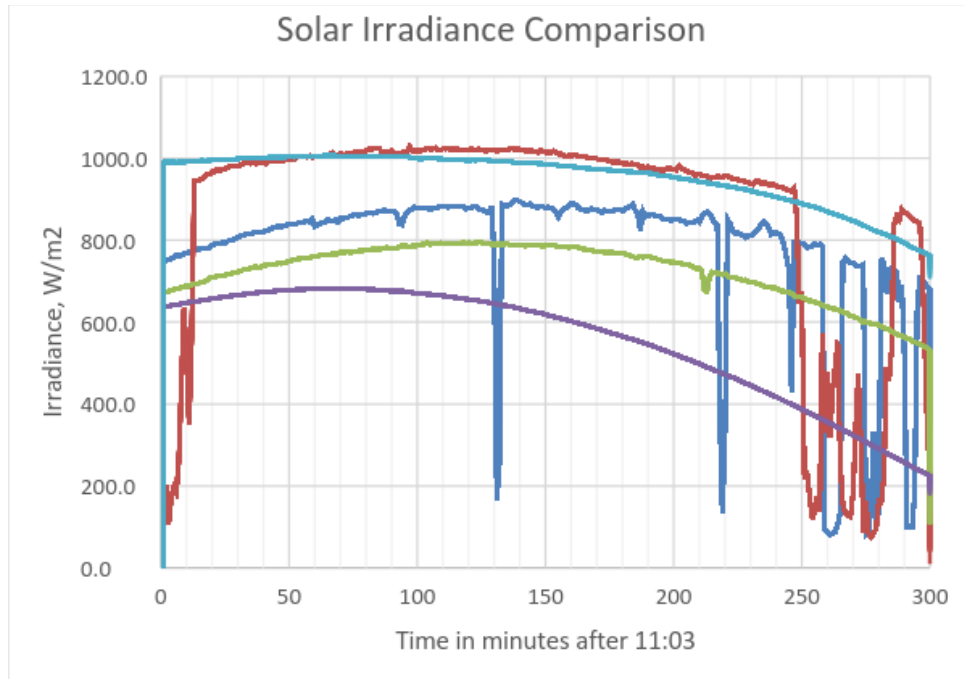


Figure 12: Solar irradiance comparison. (See explanation below).

Table 1 displays information related to the curves in Figure 12:

Table 1: Summary data of the measurements taken in Rockville and Tucson

<i>Series</i>	<i>Date</i>	<i>color</i>	<i>Pyranometer</i>	<i>Location</i>	<i>Noon Sun Altitude</i>
A	8/27/2016 10/27/201	blue	GHI	Rockville	57
B	7	red	Tracker DNI	Rockville	36.7
C	9/23/2016 11/25/201	green	GHI	Rockville	48.3
D	6 11/25/201	purple	GHI	Tucson	36.8
E	6	lt blue	Tracker DNI	Tucson	36.8

The DNI tracker data are the same data as shown in the previous figure. The tracker DNI data and the DNI data from Tucson (light blue) are similar. The Tucson data were selected from 11/25/2016 because the Sun altitude was similar to the Rockville data on 10/27/2017. The DNI data are higher than the horizontal or GHI data, because those include the cosine effect due to directivity of the pyranometer. Note that in some cases the tracker direct data are higher than the Tucson DNI data, because the pyranometer data has a wider acceptance angle than the Tucson sensor, which only looks at a very narrow angle around the Sun, and rejects additional diffuse light outside this angle.

Discussion

The original design of the Sun tracker worked well indoors, under artificial illumination from a ceiling light. However, in sunlight it performed poorly. It would either move around randomly, or get stuck at the limit of the servo motion.

It was necessary to understand the tracker's underlying principles more deeply. Since the only analog parts in the circuit were the photoresistors, we focused our attention on these. We noted that the photoresistors form part of a bridge circuit that controls the servo motion through the Arduino. Sunlight is much brighter than indoor light. A light meter held two meters from a conventional ceiling light measured about 110 lux (a unit of luminance). Sunlight in a clear sky measured over 150,000 lux – over three orders of magnitude higher. We conducted some measurements of the resistance of the photoresistor as a function of luminance in lux. A representative plot of this kind of data, for different types of photoresistors, is shown in figure 13.

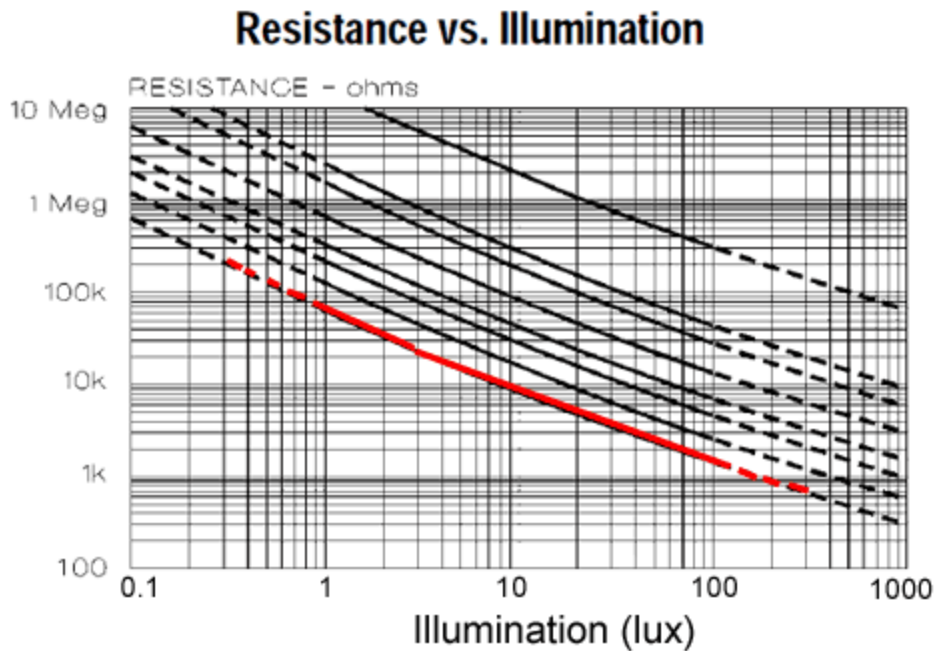


Figure 13: A Graph representing the resistance as it changes with lux.

The photoresistors in our tracker have a resistance curve similar to the red curve in this graph.

Note that the resistance decreases with increasing sunlight. At very high illumination levels, the resistance will be very low, causing the circuit to operate far outside its designed range.

To remedy this situation, we added two photoresistors in series to each of the four light sensors, to increase the resistance. However, this did not appreciably improve its tracking ability in sunlight.

Then, we added a filter – “sunglasses” -- on the front of the photoresistors, sufficient to move their resistance into the operating range under sunlight. This required a very dark filter: an unexposed black 35mm slide film. Pieces of this film were glued to the front of the four photoresistors. This modification resulted in good tracking performance in sunlight.

A photograph of the tracker in operation in figure 14. (It is on top of a “Stevenson box” used to house instruments temporarily. In practice the tracker will be placed far away from the anemometer).



Figure 14: Sun tracker resting atop the Stevenson box. The pyranometer is mounted on the tracker. Two photoresistors are visible in front of the black plates.

Conclusions

The comparisons in Figure 12 show that the tracker is giving measurements that are as expected. In the future, the tracker will be packaged in a robust structure for routine use and protection from weather.

This instrument will serve to automate and improve the accuracy of solar cooker standard power measurements. This in turn will enable more reliable and reproducible measurements in accordance with the standard anywhere in the world.

Acknowledgements

Instruments and editorial guidance in preparation of this report were provided by Solar Household Energy, Inc. The authors wish to give great appreciation to Ms. Angelique Bosse, Montgomery Blair Magnet Srp. for introducing the authors.

References

1. E. Rehfuss et al., 2006. “Assessing household solid fuel use: multiple implications for the Millennium Development Goals”. *Environ Health Perspectives* 114, 373–378.
 2. Energy and Air Pollution 2016 - World Energy Outlook Special Report p. 13,
<http://www.iea.org/publications/freepublications/publication/weo-2016-special-report-energy-and-air-pollution.html>
 3. "Five Years of Impact: 2010-2015", Global Alliance for Clean Cookstoves,
<https://cleancookstoves.org/about/our-mission/>
 4. “ISO TC 285 Cookstove Standards Update”,
<http://www.pciaonline.org/webinars>
 5. ISO-19867-1, “Clean cookstoves and clean cooking solutions, Part 1”,
http://www.iso.org/iso/catalogue_detail.htm?csnumber=66519
 6. “How to Participate in the Standards Process”,
<http://cleancookstoves.org/technology-and-fuels/standards/how-toparticipate.html>
 7. Solar Cookers International Network,
<http://solarcooking.wikia.com/>
 8. “New Cooking Bag”, <http://www.new-cooking-bag.com/>
 9. Sun or Moon Altitude/Azimuth Table
<http://aa.usno.navy.mil/data/docs/AltAz.php>
 10. “Testing and Reporting Solar Cooker Performance”, American Society of Agricultural and Biological Engineers, ASABE S.580.1, Nov. 2013.
<http://www.asabe.org/media/200979/s580.1.pdf>
 11. “Arduino Sun Tracker Turret”, Hackster.io community
<https://www.hackster.io/robotgeek-projects-team/arduino-sun-tracker-turret-06cba9>
- NOAA Solar Position Calculator
<https://www.esrl.noaa.gov/gmd/grad/solcalc/azel.html>
- Solar Resource & Meteorological Assessment Project (SOLRMAP)
Observed Atmospheric and Solar Information System (OASIS)
University of Arizona, Tucson, Arizona
http://midcdmz.nrel.gov/ua_oasis/

David R. Brooks
Institute for Earth Science Research and Education
<http://www.instesre.org/>

Measuring Sunlight at Earth's Surface: Build Your Own Pyranometer, David Brooks, PhD,
Institute for Earth Science Research and Education (February, 2007)
<http://www.instesre.org/construction/pyranometer/pyranometer.htm>

Apogee SP-212 Amplified Pyranometer
<https://www.apogeeinstruments.com/sp-212-amplified-0-2-5-volt-pyranometer/>

Glossary of Solar Radiation Resource Terms
http://rredc.nrel.gov/solar/glossary/gloss_a.html

Clear sky radiation equation from
ASCE Standardized Reference Evapotranspiration Equation
<http://www.kimberly.uidaho.edu/water/asceewri/index.html>